J Mater Sci: Mater Med (2008) 19:2589–2594
DOI 10.1007/s10856-007-3241-0

Intraosseous pressure and strain generated potential of cylindrical bone samples in the drained uniaxial condition for various loading rates

Junghwa Hong · Sang Ok Ko · Gon Khang · Mu Seong Mun

Received: 27 February 2007 / Accepted: 16 July 2007 / Published online: 4 October 2007

Abstract Cortical bone is a composite material consisting of a porous elastic solid and viscous fluid. It is well known that the intraosseous fluid circulates as a result of a bone fluid pressure gradient in the porous space of the cortical bone. When a time-dependent mechanical load is applied to the bone, intraosseous fluid flow occurs through the interconnected pore space in the bone. Bone fluid flow leads to a strain generated streaming potential (SGP). However, there is no experimental study on the relationship between the generation of intraosseous pressure and the SGP. The purpose of this study was to obtain the relationship between SGP and intraosseous pressure generations in cortical bone. In order to understand the issue, a drained, one-dimensional experimental setup for fluid-filled cortical bone samples with four different strain rates was used to simultaneously measure the intraosseous pressure and SGP. The results revealed a significant correlation ($r = 0.98$, $p = 0.02$) between the generation of the SGP and the intraosseous pressure, which indicates that an intraosseous pressure gradient produces a SGP in cortical bone.

J. Hong (✉) · S. O. Ko
Biomechatronics Laboratory, Department of Control and Instrumentation Engineering, Korea University, 208 Seochang-Ri, Jochiwon-Eup, Youngi-Gun, Chungnam 339-700, Republic of Korea
e-mail: hongjh32@korea.ac.kr

G. Khang
Department of Biomedical Engineering, Kyung Hee University, 1 Seochun-Ri, Kihung-Eup, Youngin-City, Gyeonggi 449-701, Republic of Korea

M. S. Mun
Korea Orthopedics and Rehabilitation Engineering Center, Incheon, Republic of Korea

1 Introduction

Bone is a composite material consisting of a porous elastic solid and viscous fluid. The viscous fluid in the bone occupies the space outside the blood vessels and nerves in the Volkmann and osteonal canals, as well as in the extracellular space in the lacunae and the canaliculi [1]. It was reported that the viscosity of intraosseous fluid in the cortical bone is approximately equal to the viscosity of physiological saline [1]. In contrast, the viscosity of intraosseous fluid in the cancellous bone of cattle is 0.07 Pa-s, which is approximately 67 times the viscosity of physiological saline at 37 °C [2]. It is well understood that the intraosseous fluid circulates as a result of the bone fluid pressure gradient in the porous space of the bone [3–11], which is known to be continuous [12]. Recent reports also support fluid flow in the bone. One study reported that an external mechanical load macroscopically enhances the intramedulary pressure significantly [13]. An ex-in vivo study using an amputated sheep forelimb reported the existence of intraosseous fluid flow in the cortical bone after applying a 0.2% of peak strain pulse [14]. These recent experimental results confirmed the generation of intraosseous pressure that induces flow. Wang et al. [15] reported the presence of intraosseous fluid flow in the bone in vivo. In addition, theoretical models have suggested and predicted the flow of fluid, even in the lacunocanalicular level to support fluid induced mechanosensation on the connected cellular network [16, 17]. The studies strongly support the existence of intraosseous fluid flow as well as an osseo-remodeling mechanism by the bone fluid.

Intraosseous fluid flow is closely related to the bone strain generated potential. An electrical charge is generated in the presence of electrical double layers on the cells and surfaces of the bone matrix [18]. As bone cells are

negatively charged, a very thin layer of fluid near the surface of the cells becomes positively charged [19]. When a time-dependent nonuniform mechanical load is applied to the fluid-filled bone, intraosseous fluid flow occurs through the interconnected pore space in bone. The bone fluid flow will then lead to movement of this charged layer of fluid, which causes an electrical field in the bone tissue. This phenomenon is known as the bone strain generated streaming potential (SGP). Bone tissue with intraosseous fluid flow can have an electric potential regardless of whether it is alive or not [20, 21]. In general, the bone SGP is affected by the viscosity, flow rate, and intraosseous pressure distribution. For example, the bone SGP resulting from the flow of bone fluid has a low flow rate if the viscosity of the fluid is high and the potential decreases as a consequence.

It has been suggested that bone SGP affects the bone remodeling process [22]. The intensity of the electric potential in the bone tissue decreases when there is a lesion, and there is a remarkable electric potential when bone tissue is formed again in a fractured part. In addition, a negative potential increases in the epiphyseal growth plate when the bone tissue grows faster. Ultimately, the SGP controls the activity of osteoblasts, stimulates osteogenesis on the negative pole, and promotes bone resorption on the positive pole [23, 24]. Harrigan and Hamilton [25] proposed a model for the occurrence of SGP difference as a result of the flow of bone fluid using the theory of poroelasticity. MacGinitie et al. [26] carried out four-point bending experiments with specimens collected from a section of cattle femur in order to determine the relationship between fluid flow and the SGP. Beck et al. [27] suggested a relationship between stress and the SGP by performing compression and bending experiments with the ulna of turkeys. In this way, a SGP occurs in the bone tissue deformed by an external force applied under various conditions and it is known to be related to bone growth or remodeling. However, all studies on the SGP assumed or theoretically predicted that intraosseous fluid flow induced the generation of SGP in bone.

As reviewed, the application of an external load causes intraosseous fluid flow and the generation of SGP in bone. Due to technical difficulties, simultaneously quantifying loading-induced intraosseous pressure and SGP generation has not been performed. As a result, there are no reports on the relationship between the intraosseous pressure and the SGP. The purpose of this study was to obtain the relationship between SGP and intraosseous pressure generations in cortical bone. In order to understand the issue, a drained one-dimensional experimental setup for fluid-filled cortical bone samples in vitro was proposed. This experimental setup induced intraosseous fluid flow to the loading direction only. The intraosseous pressure and level of SGP generation in the bone samples at various strain rates were measured simultaneously.

2 Materials and methods

A total of 16 cylindrical cortical bone samples from 16 fresh bovine femoral diaphyses were fabricated using a micro-milling machine with a resolution of 10 μm (EGX-300, Roland, Japan). The specimens were, on average, 22 weeks old and had a mean weight of 215 kg at the time of death. Based on the proximal-to-distal direction, a 10 mm diameter and 10-mm long cylindrical sample was obtained at the lateral-middle side of the femoral diaphysis as shown in Fig. 1a. Since the diameter of the specimen was 10 mm, the possible fabricating error by the micro-milling machine was about 0.2%. The accuracy of fabrication of the samples was carefully examined by an optical microscope (NAVITAR, USA) with an image processor (HITACHI, Japan). The system had a resolution of 5 μm when a field of view was 10 mm. The preparations were performed while the specimens were frozen in order to minimize the loss of bone fluid and the damage artifact [28]. A plane radiograph was taken in order to exclude any samples with structural defects. After fabrication, the specimens were reserved in saline soaked gauze to minimize the loss of bone fluid, and then stored in plastic bags at –20 °C.

To represent one-dimensional flow, the flow of intraosseous fluid across the radial and axial bottom boundaries of the cylindrical bone sample was not permitted. Therefore, the intraosseous fluid could flow out through the axial upper boundary of the bone sample. The condition of uniaxial strain was applied in order to allow only axial deformation in the bone sample. A testing apparatus was specially designed for this purpose, as illustrated in Fig. 1b. A very stiff stainless steel annulus having a diameter of 9.95 mm and a length of 10 mm and solid porous loading piston provided the drained uniaxial strain condition by restricting the lateral deformation and fluid flow and allowing axial deformation and fluid flow. The diameter of annulus was less than that of the samples to use a tight fitting method when the samples were inserted into the hole. The porous loading platen allowed the leakage of intraosseous fluid during the tests. A pressure transducer (S11-M2, Primo, Japan) located at the bottom of the bone sample was used to monitor the generation of intraosseous pressure through a small hole (a diameter of 2 mm) on the bottom of the apparatus. The sensitivity of the pressure transducer was 56 mV/Pa. The transducer can detect pressure as low as 0.2–2.0 Pa [29]. The pressure transducer was connected to an amplifier (DA-1602; CAS, Korea) with the set output voltage ranging from 0–5 V.

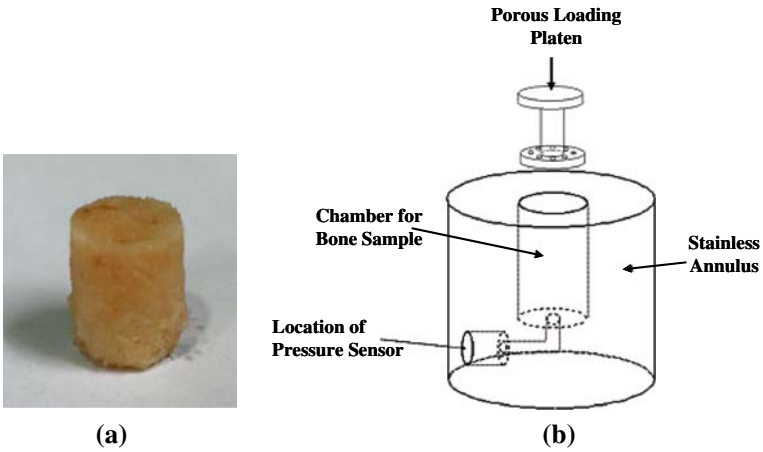

Fig. 1 A bovine femoral cortical bone sample (**a**) and schematic diagram of the drained uniaxial strain test apparatus (**b**)

A frozen bone sample was positioned using a tight fitting to minimize a possible gab between the annulus wall and bone surface and thawed in the chamber of the apparatus. In order to minimize the loss of bone fluid, a latex rubber membrane was used to seal the top of the chamber during thawing. Thawing to room temperature (20 °C) was completed within 2 h. After thawing, the porous loading piston was inserted into the chamber. The apparatus containing the bone sample and the piston was submerged in a reservoir filled with physiological saline. The reservoir was located in a vacuum chamber to remove all the air in the bone samples and the apparatus. As a result, the bone samples and the apparatus were saturated with bone fluid and saline.

The differential configuration of the amplifiers (AD620, ANALOG DEVICE, USA) with a total of five probe type electrodes was used to eliminate all the common mode noises for measuring the SGP. As shown in Fig. 2a, insulated electrodes with only the tip exposed were used to measure the SGP. As a result, only the exposed tip could sense the SGP when the insulated electrode was inserted into the bone sample. Four insulated electrodes were inserted into the bone sample in order to determine the spatial SGP variation in the axial direction of the bone sample, as indicated in Fig. 2b. In addition, one reference electrode was located on the top of the bone sample.

After instrumentation for measuring the intraosseous pressure and SGP, the instrumented apparatus was mounted on a servo material-testing machine (Kyungsung, Republic of Korea), as shown in Fig. 3. The bone samples were subjected to strain of 0.5%, which is less than the elastic range of cortical bone. Compression tests in the drained uniaxial strain condition were performed at the following four different strain rates: 0.01, 0.05, 0.1 and 0.5/s, using the four bone samples for each strain rate. The measured SGP variation and intraosseous pressure at a sampling rate of 2,000 samples/s were saved on a PC through a 12 bit A/D converter (PCI-6071E, National Instrument, USA) with BNC-2110 (National Instrument, USA).

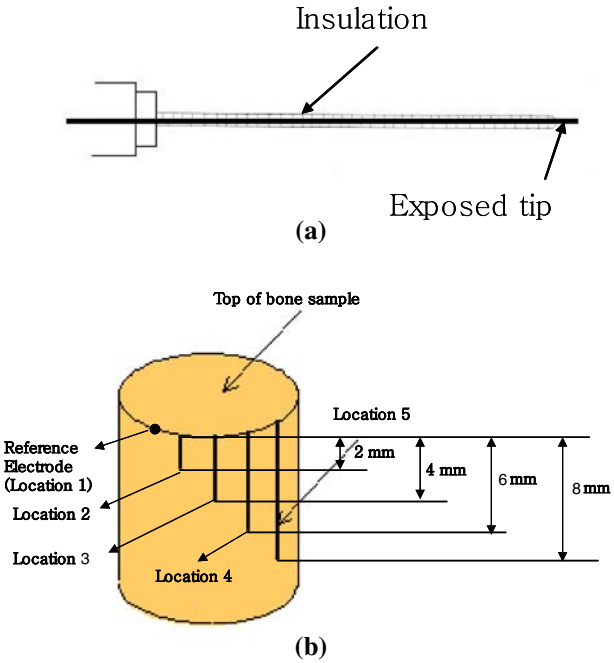

Fig. 2 Insulated AgCl electrodes with only the tip exposed used for the measurement of SGP (**a**) and measurement locations of SGP in the axial direction of the bone sample (**b**)

3 Results

Figure 4 shows the changes in the average maximum intraosseous pressure at the bottom of the bone samples as a function of the strain rate. In general, the level of intraosseous pressure generated increased with increasing applied strain rate. The mean maximum intraosseous pressure values ± standard deviations at strain rates of 0.01, 0.05, 0.1 and 0.5/s, were 7.86 ± 1.63, 10.93 ± 1.61,

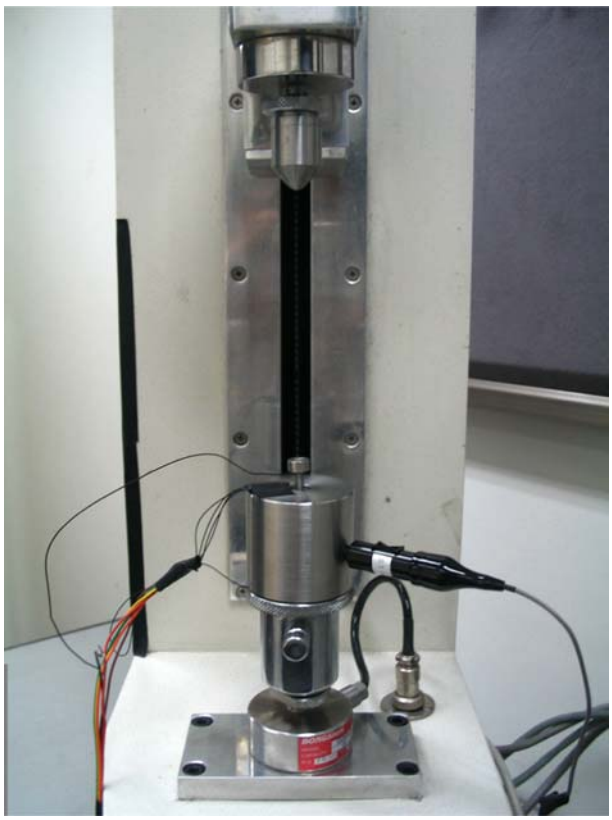

Fig. 3 Experimental setup in the drained uniaxial condition for measuring the SGP and intraosseous pressure as a function of the strain rate

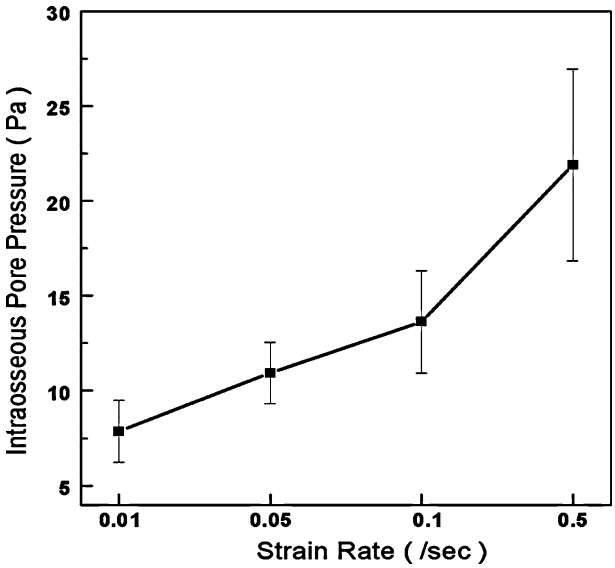

Fig. 4 Changes in the averaged maximum intraosseous pressure at the bottom of the bone samples as a function of the strain rate (0.01, 0.05, 0.1, and 0.5 per second). The error bars indicate the standard deviations with a sample size of four for each strain rate

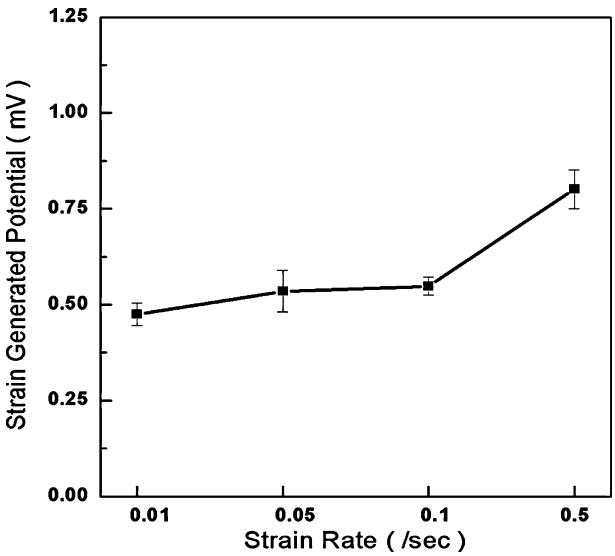

Fig. 5 Changes in the averaged maximum SGP at the measurement location five that was near the bottom of the bone samples as a function of the strain rate (0.01, 0.05, 0.1, and 0.5 per second). The error bars indicate the standard deviations with a sample size of four for each strain rate

13.63 ± 2.69, and 21.9 ± 5.05 Pa, respectively. ANOVA revealed significant differences ($p < 0.001$) in the mean maximum intraosseous pressure values between the four different strain rates.

Figure 5 shows the changes in the average maximum SGP at measurement location five, which was at the near the bottom of the bone samples with the variation in the strain rate. A similar SGP behavior to the generation of intraosseous pressure was observed with the variation in the strain rate. The SGP value increased with increasing applied strain rate. The mean maximum SGP values ± standard deviations at strain rates of 0.01, 0.05, 0.1 and 0.5/s, were 0.474 ± 0.029, 0.535 ± 0.054, 0.648 ± 0.023, and 0.801 ± 0.051 mV, respectively. ANOVA revealed significant differences ($p < 0.007$) in the average maximum SGP values between the four different strain rates. The average maximum intraosseous pressure and SGP values at the bottom of the bone samples at strain rates of 0.01, 0.05, 0.1 and 0.5/s were significantly correlated ($p = 0.02$). Pearson correlation coefficient was 0.98.

Figure 6 shows the changes in the average maximum spatial SGP variations in the axial direction of the bone sample as a function of the strain rate. Table 1 represents the detailed results. The highest mean maximum spatial SGP variation was observed at the fastest strain rate (0.5/s). In contrast, the lowest mean maximum spatial SGP variation was observed at the slowest strain rate (0.01/s). In general, the curves of the mean maximum spatial SGP variation in the axial direction increased with increasing applied strain rate. ANOVA revealed significant differences in the SGP values with variation of the strain rate ($p < 0.008$) at measurement locations 2, 3, 4, and 5. In

contrast, there was no significant difference observed at location one.

4 Discussion

External loading to the bone during physiological activity causes dynamic deformation of the bone tissue. The dynamic deformation of the bone tissue interacts with the intraosseous fluid. The mechanical interaction generates an intraosseous pressure gradient, which is a major source of fluid flow in the bone. Based on the poroelasticity, a mechanical loading to fluid-saturated bone causes an intraosseous fluid pressure gradient [1]. The characteristics of the intraosseous fluid pressure in the bone are a function of its poroelastic properties and boundary conditions. The most important factor governing intraosseous fluid flow is the fluid and loading boundary conditions. An undrained condition shows that the intraosseous fluid can be totally prevented from flowing out of the bone sample across the boundary. A drained condition is that the intraosseous fluid can flow across the boundary. As indicated in a previous study [30], the undrained fluid boundary causes the generation of the most extreme intraosseous fluid pressure in the bone without intraosseous fluid flow. In contrast, the time dependent poroelastic behavior of the bone occurs as a result of intraosseous fluid flow in the drained condition. The characteristics of intraosseous fluid flow in the drained condition are mainly affected by the permeability coefficient of the bone and external loading rate as well as the morphology of the fluid boundary [5].

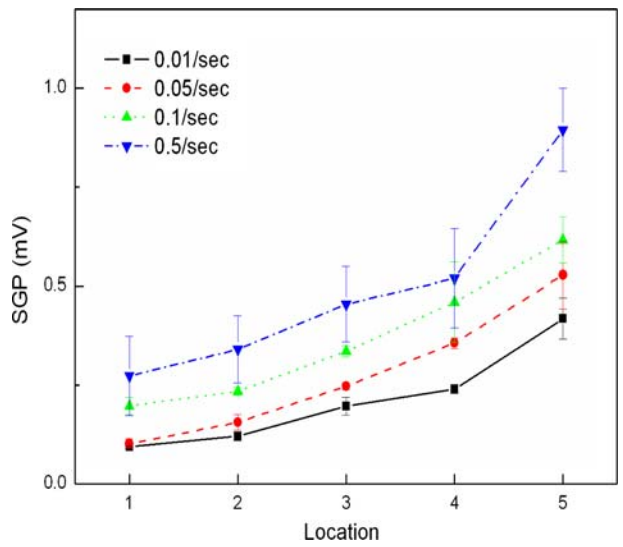

Fig. 6 Changes in the averaged maximum spatial SGP variations in the axial direction of the bone sample as a function of the strain rate (0.01, 0.05, 0.1, and 0.5 per second). The error bars indicate the standard deviations with a sample size of four for each strain rate

The highest physiological strain rate is approximately 0.1/s [30]. In this study, the intraosseous pressure obtained at the bottom of the cortical bone samples was approximately 14 Pa at the strain rate, which is very low. In this study, the bovine cortical bone samples were obtained from the femoral diaphyses in the direction of proximal-to-distal (long axes of bone). In these samples, the Haversian canals that are cylindrical structures of a radius of approximately 125 μm [31] lie roughly along the direction of the axial deformation and fluid flow of the bone samples. Since the Haversian canals are connected with the Volkmann's canals transversely, all canals in the cortical bone are interconnected. In addition, the fluid boundary condition on the top of the specimens allows free flow through the boundary. As a result, it can be considered that the intraosseous fluid can flow through the pipes (Haversian and Volkmann's canals) with relatively small hydraulic resistance (high permeability) with a relatively large diameter. However, the fluid boundary condition of the cortical bone in the long bone would be different from those used in this study because the structure is much larger than the bone samples and the Haversian canals are not open to the outside. Therefore, there would be greater resistance to intraosseous fluid flow than those shown in this study. It was suggested that the generation of intraosseous pressure in cortical bone in the long bone in vivo would be larger than the results in this study suggest.

As shown in Fig. 4 and 5, the changes in intraosseous pressure at the bottom of the cortical bone samples as a function of the strain rate show a similar behavior of the SGP. The correlation between the intraosseous pressure and SGP behavior was statistically significant ($r = 0.98$, $p = 0.02$). Therefore, the intraosseous pressure gradient produces the SGP. In addition, the amount of an intraosseous pressure gradient governs the production of SGP. Based on the analytical model, which was same as the experimental setup used in this study [5], the generation of intraosseous pressure is a function of the location in a cancellous bone sample. The intraosseous pressure decreases as the location is closed to the drained boundary. As shown in Fig. 6, the measured SGP became large at all strain rates when the measurement location was moved to the bottom of the cortical bone sample. Therefore, these results show that the SGP is governed by the intraosseous pressure gradient, the amount intraosseous fluid flow.

In this study, the simultaneous measurement of the loading-induced intraosseous pressure and SGP was performed for the first time. A drained one-dimensional experimental setup for the fluid-filled cortical bone sample was used. In any case, the relationship between the intraosseous pressure and the SGP was understood even though limited conditions were examined. However, the characteristics of the intraosseous pressure in vivo will be very

Table 1 Variation of the averaged maximum spatial SGP variations in the axial direction of the bone sample as a function of the strain rate (0.01, 0.05, 0.1, and 0.5 per second)

Location	SGP ± Standard deviation			
	Strain rate of 0.01	Strain rate of 0.05	Strain rate of 0.1	Strain rate of 0.5
1	0.082 ± 0.03	0.112 ± 0.021	0.134 ± 0.035	0.204 ± 0.018
2	0.104 ± 0.026	0.143 ± 0.037	0.229 ± 0.029	0.328 ± 0.049
3	0.185 ± 0.034	0.226 ± 0.032	0.329 ± 0.047	0.452 ± 0.047
4	0.276 ± 0.025	0.353 ± 0.029	0.465 ± 0.03	0.558 ± 0.086
5	0.474 ± 0.029	0.535 ± 0.054	0.548 ± 0.023	0.801 ± 0.051

Unit: SGP (mV), and Strain rate (/s)

different from that obtained in this study. It is still open question as to how much the amount of intraosseous pressure generation and SGP in the cortical bone could be measured in the physiological condition, in vivo.

Acknowledgements This work was sponsored by the Special Research Center Support Program of Medical Devices and Supplies Development Grants (A020603) of Korean Ministry of Health and Welfare.

References

1. S. C. COWIN, *J. Biomech.* **32** (1999) 217
2. J. D. BRYANT, T. DAVID, P. H. GASKEIL, S. KING and G. LOND, *Proc. Inst. Mech. Eng. [H]: J. Eng. Med.* **203** (1989) 11
3. K. PIEKARSKI and M. MUNRO, *Nature* **269** (1977) 80
4. A. F. MAK, D. T. HUANG, J. D. ZHANG and P. TONG, *J. Biomech.* **30** (1997) 11
5. T. H. LIM and J. H. HONG, *J. Musculoskeletal Res.* **2** (1998) 167
6. J. L. NOWINSKI and F. C. DAVIS, *Math. Biosci.* **8** (1970) 397
7. J. L. NOWINSKI, *Acta Mech.* **13** (1972) 281
8. J. A. OCHOA, A. P. SANDERS, D. A. HECK and B. M. HILLBCRRY, *J. Biomech. Eng.* **113** (1991) 259
9. J. A. OCHOA and B. M. HILLBERRY, *Trans. Orthop. Res. Soc.* **17** (1992) 163
10. S. WEINBAUM, S. C. COWIN and Y. ZENG, in "Advances in Bioengineering", edited by R. Vanderby Jr. (American Society of Mechanical Engineers, New York, 1991) p. 317
11. D. ZHANG and S. C. COWIN, *J. Mech. Phys. Solids* **42** (1994) 1575
12. S. HUGHES, R. DAVIES, R. KHAN and P. KELLY, *Clinl. Orthop. Relat. Res.* **134** (1978) 332
13. J. NAGATOMI, B. P. ARULANANDAM, D. W. METZGER, A. MEUNIER and R. BIZIOS, *J. Biomech. Eng.* **123** (2002) 308
14. T. M. L. KNOTHE and U. KNOTHE, *J. Biomech.* **33** (2000) 247
15. L. WANG, C. CIANI, S. B. DOTY and S. P. FRITTON, *Bone* **34** (2004) 499
16. S. WEINBAUM, S. C. COWIN and Y. ZENG, *J. Biomech.* **27** (1994) 339
17. R. M. DILLAMAN, R. D. ROER and D. M. GAY, *J. Biomech.* **24**(S1) (1991) 163
18. S. C. COWIN, L. MOSS-SALENTIJN and M. L. MOSS, *J. Biomech. Eng.* **113** (1991) 191
19. J. A. SPADARO, in "Bone", edited by B. K. Hall (CRC Press, Boca Raton, Florida, 1993) p. 37
20. D. GROSS and W. S. WILLIAMS, *J. Biomech.* **15** (1982) 277
21. D. PIENKOWSKI and S. R. POLLACK, *J. Orthop. Res.* **1** (1983) 30
22. S. R. POLLACK, in "Bone Mechanics Handbook", edited by S. C. Cowin (CRC Press, Boca Raton, Florida, 2001) pp. 21–24
23. C. A. BASSETT and R. O. BECKER, *Science* **137** (1962) 1063
24. R. B. BORGENS, *Science* **225** (1984) 478
25. T. P. HARRIGAN and J. J. HAMILTON, *J. Biomech.* **26** (1993) 183
26. L. A. MACGINITIE, G. D. STANLEY, W. A. BIEBER and D. D. WU, *J. Biomech.* **30** (1997) 1133
27. B. R. BECK, Y-X. QIN, K. J. MCLEOD and M. W. OTTER, *Calcif. Tissue Int.* **71** (2002) 335
28. T. M. KEAVENY, X. E. GUO, E. F. WACHTEL, T. A. MCMAHON and W. C. HAYES, *J. Biomech.* **27** (1994) 1127
29. K. WATANABE, T. WATANABE, H. WATANABE, H. ANDO, T. ISHIKAWA and K. KOBAYASHI, *IEEE Trans. Biomed. Eng.* **52** (2005) 2100
30. J. H. HONG, *Proc. Inst. Mech. Eng. [H]: J. Eng. Med.* **218** (2004) 375
31. R. R. COOPER, J. W. MILGRAM and R. A. ROBINSON, *J. Bone Joint Surg.* **48A** (1966) 1239